Journal of Controlled Release 328 (2020) 160–170

Contents lists available at ScienceDirect

Journal of Controlled Release

journal homepage: www.elsevier.com/locate/jconrel

Overcoming resistance to rituximab in relapsed non-Hodgkin lymphomas by antibody-polymer drug conjugates actively targeted by anti-CD38 daratumumab

Ondřej Lidický[a,1], Pavel Klener[b,c,a,1], Daniela Machová[a], Petra Vočková[b,c], Eva Pokorná[b], Karel Helman[d], Cory Mavis[e], Olga Janoušková[a], Tomáš Etrych[a,*]

[a] Institute of Macromolecular Chemistry, Academy of Sciences of the Czech Republic, Heyrovský Sq. 2, 162 06 Prague 6, Czech Republic
[b] Institute of Pathological Physiology, First Faculty of Medicine, Charles University, U Nemocnice 5, 128 53 Prague 2, Czech Republic
[c] First Department of Internal Medicine- Hematology, University General Hospital and First Faculty of Medicine, Charles University, U Nemocnice 2, 128 08 Prague 2, Czech Republic
[d] Faculty of Informatics and Statistics, University of Economics, Prague, Czech Republic
[e] Department of Medicine Lymphoma/Myeloma, Roswell Park, Comprehensive Cancer Center, Elm & Carlton Sts, Buffalo, NY 14263, United States of America

ARTICLE INFO

Keywords:
Non-Hodgkin lymphoma
Active targeting
Drug delivery
APDC
Polymer nanomaterials
Rituximab
Daratumumab
CD38

ABSTRACT

B-cell non-Hodgkin lymphomas (B-NHL) represent the most common type of hematologic malignancies in the Western hemisphere. The therapy of all B-NHL is based on the combination of different genotoxic cytostatics and anti-CD20 monoclonal antibody (mAb) rituximab. Unfortunately, many patients relapse after the mentioned front-line treatment approaches. The therapy of patients with relapsed/refractory (R/R) B-NHL represents an unmet medical need. We designed, developed and tested novel actively targeted hybrid mAb-polymer-drug conjugate (APDC) containing anti-CD20, anti-CD38 or anti-CD19 mAbs. Biocompatible copolymers based on N-(2-hydroxypropyl)methacrylamide (HPMA) with cytostatic agent doxorubicin attached via stimuli-sensitive hydrazone bond were employed for the mAb grafting. Anti-lymphoma efficacy of the APDC nanotherapeutics was evaluated in vivo on a panel of three patient-derived lymphoma xenografts derived from two patients with R/R B-NHL and one patient with so far untreated B-NHL. In both PDX models derived from patients with R/R B-NHL, the targeting with anti-CD38 antibody daratumumab demonstrated highly improved anti-lymphoma efficacy compared to the targeting with anti-CD20 rituximab, two experimental anti-CD19 antibodies and non-targeted controls. The results represent a proof-of-concept of a new algorithm of personalized anti-tumor therapy based on highly innovative APDC biomaterials.

1. Introduction

Non-Hodgkin lymphomas (NHL), the most common hematologic malignancies, are heterogeneous lymphoid tumors of immune cells [1,2]. Current front-line therapy is based on diverse immunochemotherapy regimen, e.g. CHOP (C-cyclophosphamid, H-doxorubicin, O-oncovin, P-prednisone) in combination with anti-CD20 antibody rituximab (R-CHOP) [3–5]. Rituximab is a chimeric monoclonal antibody (mAb) targeting surface CD20 antigen presented on normal mature B-cells and virtually all lymphoma cells of B-cell origin [6]. After cell surface opsonization by rituximab several mechanisms lead to lymphoma cell death including Direct Cell Death (DCD), Antibody Dependent Cell Cytotoxicity (ADCC) and Complement-Dependent cell Cytotoxicity (CDC) [7]. While DCD is triggered by binding of the mAb to CD20 antigen, ADCC and CDC depend on Fc fragment-mediated activation of the complement cascade and immune cells, respectively. Natural killer cells and macrophages belong to major effector cells of ADCC. Despite the fact that the outcome of patients with B-NHL improved considerably during the last 20 years, approximately half of all patients experience relapse after achievement of remission [8]. Such patients are subject to diverse chemotherapy salvage regimens that implement different cytostatics, e.g. platinum derivatives and high-dose cytarabine [9,10]. In most instances these different chemotherapy regimens are combined with the same anti-CD20 antibody rituximab [9]. General usage of rituximab in the relapse setting is a consequence of two facts: first, despite the fact that a proportion of patients might

* Corresponding author.
E-mail address: etrych@imc.cas.cz (T. Etrych).
[1] Both authors contributed equally.

https://doi.org/10.1016/j.jconrel.2020.08.042
Received 16 June 2020; Received in revised form 11 August 2020; Accepted 21 August 2020
Available online 27 August 2020

present with CD20-negative disease by standard immunohistochemistry after failure of rituximab-based upfront therapy, not all patients are subject to lymphoma re-biopsy at the time of relapse. And second, despite a number of trials there is currently no effective immunotherapy approved for the treatment of relapsed B-NHL other than anti-CD20 antibodies (namely rituximab, ofatumumab and obinutuzumab) [11,12]. Nevertheless, some other CD molecules, such as CD19, CD22, CD38 and CD79b, remains highly interesting targets for the advanced B-NHL treatment within future development [13,14].

To improve anticancer drug efficiency a variety of drug delivery systems (DDS) have been studied. In June 2019, FDA approved accelerated approval for the Antibody Drug Conjugate (ADC) polatuzumab-vedotin (anti-CD79b mAb conjugated with mitotic toxin monomethyl auristatin E) for the therapy of R/R diffuse large B-cell lymphoma (DLBCL), the most prevalent type of lymphoma in the western hemisphere [15,16]. ADCs, however, rely on small cytotoxic molecules with potent systemic toxicity, e.g. anti-mitotic agents, and their anti-lymphoma activity is mediated by the mAb-mediated targeted delivery of the toxins to the lymphoma cells. Apart from ADCs, also other nano-sized DDS can help to overcome insolubility of hydrophobic drugs, prolong the time of circulation in the bloodstream, minimize the side-toxicity and increase drug concentration in the tumor tissue thanks to the enhanced permeability and retention (EPR) effect [17]. Moreover, passive accumulation of DDS in the tumor tissue can be enhanced by various targeting moieties including monoclonal antibodies and their fragments, saccharides, lectins, (oligo)peptides etc. [18,19]. Synthetic biocompatible polymers could be used in these actively targeted DDS instead of the linker (used in the concept of ADC for controlled release of carried drugs) with multiple binding sites for the drug attachment and thus scale up the loading capacity of ADC up to ten times [20].

The most frequently used techniques for polymer attachment to antibodies [21,22] are based on the aminolytic reaction between amino groups of mAb with aminoreactive groups of synthetic polymers. Unfortunately, the involvement of amino group of mAb, either from lysine residues or N-terminal, often leads to reduction of binding activity of the mAb. Recently, for the mAb-polymer construct formation the reaction of the thiol groups introduced to the antibody with the maleimides presented in the synthetic polymer structure, so called Michael addition, has been studied widely [23,24]. Actively targeted hybrid polymer-mAb system containing therapeutic anti-CD20 mAb [20,25] combined with biocompatible polymer based on N-(2-hydroxypropyl) methacrylamide (HPMA) with attached doxorubicin via enzymatically cleavable oligopeptide spacer (GFLG) or pH-labile hydrazone bond was described [26,27]. The polymer-mAb systems with a star-like structure, in which several polymer grafts are attached to the central monoclonal mAb, enable a much higher loading capacity of carried drug when compared to the ADC [24,28]. It was shown that HPMA copolymer-bound doxorubicin has considerably reduced non-specific toxicity including hepatotoxicity, nephrotoxicity, cardiotoxicity and myelotoxicity [29]. Even within the compassionate use of polymer-pirarubicin conjugate in human reduced cardiotoxicity was proved [30].

Here we designed, synthesized and tested physico-chemical properties and in vitro and in vivo anti-lymphoma efficacy of precisely designed and synthesized HPMA-based copolymers targeted with anti-CD20 mAb rituximab, two anti-CD19 experimental antibodies and anti-CD38 mAb daratumumab in experimental therapy of CD20-negative patient-derived lymphoma xenografts derived from patients after failure of rituximab-based front-line therapies.

2. Material and methods

2.1. Materials

1-Aminopropan-2-ol, methacryloyl chlorid, 6-aminohexanoic acid, tert-butyl carbazate, N,N′-dicyclohexylcarbodiimide (DCC), 4,4′-Azobis (4-cyanovaleric acid) (ABIK), 4,5- dihydrothiazole-2-thiol (TT), 4-(dimethylamino)pyridine (DMPA), dimethyl sulfoxide (DMSO), *N*-(2-aminoethyl)maleimide trifluoroacetate, dimethylformamide (DMF), trifluoroacetic acid (TFA), triisopropyl silan (TIPS), *5,5′*-disulfanylbis(2-nitrobenzoic acid) (Ellman's reagent), doxorubicin hydrochloride (Dox·HCl), dithiothreitol (DTT), *5,5′*-dithiobis(2-nitrobenzoic acid) (Ellman's reagent), cysteine, ethylenediaminetetraacetic acid (EDTA), phthalaldehyde (OPA), *N,N*-diisopropylethylamine (DIPEA) were purchased from Sigma-Aldirch. 2,4,6-trinitrobenzene-1-sulfonic acid (TNBSA) was purchased from Serva. Chimeric anti-human CD20 antibody rituximab (mAb20) (MabThera®, Roche, Great Britain), human anti-human CD38 antibody daratumumab (mAb38) (Darzalex, Janssen Biotech, USA), mouse anti-human CD19 antibody clone 4G7 (mAb19) (Bio X cell, USA), mouse anti-human CD19 clone B3D (mAb19B) (ExBio, Czech Republic) and polyclonal immunoglobulins Flebogamma (Ab) (Grifols, Spain) were purified from excipients (e.g. glukose, NaCl, glycin) before conjugation by filtration using an Amicon®Ultra centrifugal filter units 30 K and reaction ITH buffer as a solvent. All other chemicals and solvents were of analytical grade. The solvents were dried and purified by conventional procedures and distilled before used. 3,3′-[4,4′-Azobis(4-cyano-4-methyl-1-oxo-butane-4,1-diyl)]bis (thiazolidine-2-thione) (ABIK-TT) was prepared as described previously [31].

2.2. Synthesis of monomers

N-(2-hydroxypropyl)methacrylamide (HPMA) was synthesized by reaction of methacryloyl chloride with 1-aminopropan-2-ol in dichloromethane in the presents of sodium carbonate as described previously [32]. *N*-(*tert*-butoxycarbonyl)-N′-(6-methacrylamidohexanoyl) hydrazine (Ma-εAh-NHNH-BOC) was synthesized by two-step syntheses. First, methacryloyl chloride was reacted with 6-aminohexanoic acid in the presence of NaOH and afterward formed 6-methacrylamidohexanoyoic acid was reacted with tert-butyl carbazate using DCC [33].

2.3. Synthesis of polymer precursors

Semitelechelic polymer precursor $\mathbf{P_{DOX}}$ containing main chain-end maleimide (MI) group and Dox connected via hydrazone bond to the side chain of polymer was prepared as described previously [34]. Briefly: semitelechelic copolymer **P*** containing main chain-end TT group and BOC-protected hydrazide groups in the side chains was prepared by free radical copolymerization of HPMA (840 mg, 5.86 mmol) and Ma-εAh-NHNH-BOC (157 mg, 0.5 mmol) monomers initiated by ABIK-TT (320 mg, 0.66 mmol) in DMSO (6 mL) under inert atmosphere in polymerization ampule [35]. Yield of the polymerization was 81% (667 mg). Content of TT groups was determined by using UV-VIS spectrophotometry on Specord 205 (Analytik Jena, Jena, Germany, ε_{305} = 10,700 $L{\cdot}mol^{-1}{\cdot}cm^{-1}$ in methanol [36]). The MI reactive group was introduced to semitelechelic polymer precursor **P*** by the aminolytic reaction of *N*-(2-aminoethyl)maleimide with the TT group [37]. The MI group content in the polymer precursors was determined by a modified Ellman's assay as the difference between cysteine concentrations before and after reaction with the MI groups of the polymer [38]. The yield of MI group introduction reached 69%. Hydrazide groups of polymer precursor **P** were deprotected by using mixture of TFA:-TIPS:distilled water in ratio 38:1:1 and characterized by using TNBSA (ε_{500} = 17,200 $L{\cdot}mol^{-1}{\cdot}cm^{-1}$) [39]. Dox·HCl was connected via hydrazone bond in methanol with acetic acid as described previously forming polymer precursor $\mathbf{P_{DOX}}$ with Dox [40]. The yield of Dox attachment reached 95%. Polymer precursors **P***, **P**, $\mathbf{P_{DOX}}$ were characterized using HPLC system, see Table 1, (Shimadzu, Kyoto, Japan) equipped with column SuperSW TSK3000 (Tosho Bioscience, Griesheim, Germany) in combination with multi-angle light scattering detector Dawn Helieos-II(Wyatt Technology Co., Santa Barbara, USA) and

Table 1
Characterization of polymer precursors.

Polymer precursor notation	M_w (g·mol^{-1})	Đ	End group[1]	Dox (wt %)	M_n/M_{UV}[2]
P*	25,600	1.64	TT	n.a.	1.36
P	28,500	1.51	MI	n.a.	1.01
P_{DOX}	57,000	1.93	MI	9.2	-[3]

[1] End groups located in the end of main polymer chain.
[2] Functionality of main chain end groups determined from the molecular weight determined from SEC (M_n) divided by the molecular weight obtained from the content of main chain end groups (M_{UV}).
[3] Functionality was not determined due to the overlap of the DOX spectra with the modified Ellman's assay.

Table 2
Characterization of the APDCs.

APDC	Targeting unit	M_w (g·mol^{-1})	Đ	Dox (wt %)	Content of mAb (wt%)	Rh (nm)
mAb19-P_{DOX}	CD19	490,000	1.4	5.0	52	11.0
mAb19B-P_{DOX}	CD19	340,000	1.1	5.0	47	11.1
mAb20-P_{DOX}	CD20	420,000	1.4	5.0	43	10.4
mAb38-P_{DOX}	CD38	460,000	1.4	4.8	53	10.9
Ab-P_{DOX}	Nonspecific	390,000	1.4	4.9	47	8.8
mAb20-P	CD20	227,000	1.1	n.a.	48	9.8
mAb38-P	CD38	236,000	1.1	n.a.	48	9.7

refractive index detector Optilab®-rEX (Wyatt Technology Co., Santa Barbara, USA).

2.4. Synthesis of antibody polymer drug conjugates (APDC)

APDC (Table 2) were prepared by reaction of MI main chain end group of polymer precursor **P_{DOX}** and free thiol groups of monoclonal IgG antibodies (anti-CD19, anti-CD 20, anti-CD 38) or serum immunoglobulin (Flebogama) reduced by DTT as previously described [24]. Briefly: solution of polymer precursor **P_{DOX}** (53.2 mg, c ~ 100 mg/mL) in phosphate buffer (pH 7.2; 0.1 M NaCl, 1 mM EDTA, bubbled with argon) was added to solution of anti-CD38 mAb reduced by DTT (71.1 mg, c ~ 5 mg/mL) in the same buffer. Semitelechelic polymers containing MI end groups reacted with the SH groups in the mAb via thiol-ene chemistry to form covalent thioester bonds. Unreacted SH groups were blocked by the ethylenmaleimid addition after the conjugation reaction. The mAb-polymer conjugate was desalted by chromatography on a G-25 column and lyophilized. Final APDC were characterized for molecular weights and hydrodynamic size using a Shimadzu HPLC system equipped with UV detector, refractive index (Optilab®-rEX, Wyatt Technology Co., Santa Barbara, USA) and multi-angle light scattering (DAWN EOS detector, Wyatt Technology Co., USA) using 0.3 M acetate buffer (pH 6.5) and a Superose™6 column. The Ab content was estimated by amino acid analysis after OPA derivatization (C-18 chromolith® colum; HPLC Shimadzu, Japan). The Dox content was estimated by UV-VIS spectrophotometry using the extinction coefficient determined for hydrazone bound Dox [41]. The amount of free thiol groups after the reduction was determined by using Ellman's reagent [42].

2.5. In vitro drug release from the polymer-dox conjugates

All APDC were incubated at 37 °C in 0.1 M phosphate/0.05 M NaCl buffers adjusted to pH 5.0, 6.5 and 7.4, mimicking the pH of the intracellular environment, extracellular tumor environment and bloodstream, respectively. The amount of total released Dox was determined using extraction of released DOX into the organic phase followed by HPLC analysis, as described previously [15], using the free Dox as standard. The final concentration of the conjugates in incubation media was equivalent to 0.5 mM DOX.

2.6. In vitro methods – cell lines

UPF4D cell line and VFN-D2 patient-derived xenograft (PDX) were both established at the Institute of Pathological Physiology, Charles University, from a malignant peritoneal effusion of a patient with DLBCL at second lymphoma relapse after failure of R-CHOP-based induction and salvage therapy containing rituximab, cisplatin and high-dose cytarabine. UPF4D and VFN-D2 thus represent “sister” models (a cell line and a PDX model) derived in parallel from one patient. Despite the fact that the primary lymphoma cells were CD20-negative, UPF4D cell line has a variable expression of CD20 with $CD20^+$ and $CD20^-$ side-populations (**Figure SI1**). CD20-negative side population was used for in vitro experiments. SU-DHL-5 and RAJI are CD20-positive lymphoma cell lines purchased from German Collection of Microorganisms and Cell Cultures, Braunschweig, Germany. Cell lines were cultivated in RPMI-1640 medium (Thermo Scientific, Prague, Czech Republic) supplemented with heat-inactivated 10% FBS for SU-DHL-5 or 15% FBS for UPF4D20- cells and penicillin (100 U/mL) and streptomycin (100 µg/mL).

2.7. Cell cytotoxicity – IC_{50}

For the in vitro cell viability assay 10^4 cells were seeded in 100 µL of media per well in 96-well flat-bottom plates (TPP, Sigma-Aldrich, Prague, Czech Republic) 24 h before adding the conjugates or control. Concentrations of the samples ranged from 0.02–10 µg/mL Dox eq. for antibody-polymer conjugates and from 0.015–5 µg/mL for free drug Dox. The cells were incubated with polymer conjugates or free drugs for 72 h. Then, 10 µL of the Alamar Blue® cell viability reagent (Thermo Scientific, Prague, Czech Republic) was added to each well and incubated for 4 h at 37 °C. The active component of the Alamar Blue reagent, resazurin, was reduced to the highly fluorescent compound resorufin by viable cells. The fluorescence of resorufin was detected on a Synergy Neo plate reader (Bio-Tek, Prague, Czech Republic) at an excitation wavelength of 560 nm and at an emission wavelength of 590 nm [34]. Untreated cells were used as controls. Each concentration was measured in triplicate in four independent experiments. IC_{50} was calculated from measured fluorescence as the concentration of the drug in which the viable cells were reduced by half.

2.8. Conjugate cell surface binding efficiency

The binding efficiency of the conjugates was evaluated using flow cytometry. Cells were washed with 0.5% BSA-PBS, and 2×10^5 cells in 50 µL of 0.5% BSA-PBS were incubated with antibodies or antibody polymer drug conjugates in concentrations 1, 10 or 100 µg/mL of antibodies or antibodies eq. for 30 min. The cells were then washed with 0.5% BSA-PBS and incubated for 30–40 min with 5 µL of APC-labeled mouse anti-human CD38 (HIT2), CD19 (4G7) or CD20 (2H7) antibody (Exbio, Prague, Czech Republic). Afterward, the cells were washed with 0.5% BSA-PBS and resuspended in 0.5 ml of 0.5% BSA-PBS with 1 µg/ml Sytox Blue reagent (Thermo Scientific, Prague, Czech Republic) for viability counts. Samples were measured using BD FACSVerse (Becton Dickinson, Franklin Lakes, NJ, USA). The binding efficacies of the mAb-targeted conjugates or mAb alone were calculated as the differences between the fluorescent intensities of the mAb-APC-labeled cells and the mAb-APC-marked cells after treatment with the mAb-targeted polymer conjugates or mAb alone. Significant differences were performed using GraphPad Prism (La Jolla, CA, USA, 5.5) and one-way Analysis of variance (ANOVA) followed by Tukey's range test.

2.9. ^{51}Cr release assay

Raji, SUDHL-5 and UPF4D were exposed in vitro to Rituximab (10 μg/mL), Daratumumab (10 μg/mL), to antibody-polymer conjugates containing antibody in the concentration 10 μg/mL, e.g. mAb20-P_{DOX} (20 μg/mL), mAb38-P_{DOX} (20 μg/mL), P (20 μg/mL) or DMSO and incubated at 37 °C and 5% CO_2 for 24 h. Subsequently, 5×10^6 viable cells were labeled with ^{51}Cr at 37 °C in 5% CO_2 for 2 h. ^{51}Cr-labeled cells were then placed in 96-well plates at a cell concentration of 10^5 cells/well (CDC assay) or 10^4 cells/well (ADCC assay). Cells were then exposed to antibodies and human serum (CDC, 1:4 dilution) or peripheral blood mononuclear cells (PBMCs) (ADCC, 40:1 effector: target ratio) for 6 h at 37 °C in 5% CO_2. ^{51}Cr release was measured as previously described [43]. PBMCs were obtained from healthy donors (IRB approved protocol CIC-016) and isolated by Histopaque-1077 ultracentrifugation of peripheral whole blood. Pooled human serum was used as the source of complement for CDC assays.

2.10. In vivo methods – immunodeficient mice

NOD·Cg-Prkdcscid Il2rgtm1Wjl/SzJ mice (referred to as NSG mice) were purchased from The Jackson Laboratory (Bar Harbor, ME, USA). All animals were housed and maintained in a pathogen-free environment in individually ventilated cages and provided with sterilized food and water. The experimental design was approved by the institutional animal care and use committee (MSMT − 32441/2018-7).

2.11. Patient-derived lymphoma xenografts (PDX)

Three PDX models, designated VFN-D2, VFN-B2 and VFN-M5, were used in the current project. Similar to the sister cell line UPF4D, VFN-D2 PDX cells have variable expression of CD20 both in course of serial re-transplantations (from primary to secondary mice), and within one biopsy suggesting posttranslational defect in CD20 expression (**Figure SI2**) due to a clonal selective pressure [11]. Several mechanisms were suggested but exact mechanism remains unclear [44,45]. We believe the loss of CD20 expression in UPF4D and VFN-D2 cells are direct consequence of previous rituximab-based therapy, but analysis of particular molecular mechanism responsible for the loss of CD20 are beyond scope of the current study. VFN-B2 was derived from patient with the first relapse of CD20-negative Burkitt lymphoma after failure of front-line rituximab-based intensified immunochemotherapy. VFN-M5 was derived from patient with so far untreated CD20-positive mantle cell lymphoma (MCL). All three PDX models are CD19- and CD38-positive (**Figure SI1**).

2.12. Experimental therapy of lymphoma-bearing mice

NSG mice were subcutaneously inoculated with 5×10^6 of PDX cells. Therapy was initiated when all mice developed palpable tumors. At day 1 (D1) the mice were stratified so that all cohorts contained animals with comparable calculated tumor volumes. Single dose therapy of APDC (5 mg/kg Dox eq.) was administered intra-venously via tail vein on D1. Tumor growth was recorded daily using three perpendicular dimensions (in millimeters) with a digital caliper. Tumor volumes were calculated using the following formula: $\pi/6 \times$ length $\times$ width $\times$ height. Observation was terminated (and experimental mice from the cohort euthanized) when grown subcutaneously tumors exceeded 2 cm in the largest diameter.

2.13. Characterization of the cell surface antigens density

The PDX cells (VFN-B2, VFN-M5, VFN-D2) and cell lines (UPF4D, SU-DHL5) were washed in staining buffer containing phosphate saline buffer (PBS) with sodium azide and 0,5% bovine serum albumin, incubated in PBS with 0,5% human immunoglobulin (Flebogamma, Griffols) to prevent non-specific bounding for 10 min at room temperature and washed again. After then the samples were stained with antibodies for 30 min and twice washed. Following fluorochrome-conjugated mAbs were used: CD19 PE (clone HIB19, BD Biosciences), CD20 (clone 2H7, BD Biosciences), CD38 (clone HIT2, BD Biosciences). Samples were analyzed by a FACSCanto (Becton Dickinson, San Jose, CA, USA). FCM results were processed with Kaluza software, version 2.1 (Beckman Coulter). Isotype-matched negative controls were used in all the assays to distinguish positive from negative cells. For surface antigen quantification we have used QuantiBRITE™ PE Quantification Kit (BD Bioscience) according to manufacturer instructions. This Kit contains test tubes with a mix of 4 types of beads, which differs by amount of surface PE signals (low, med-low, med-high, high). Counting geometric means we have performed a comparison of PE cell signals of used PDX-models and cell lines to beads with known amount of surface antigens, which also served as an interassay control.

2.14. Statistical analysis

To assess the *practical significance* of treatment effectiveness, we plotted charts with growth curves indicating group mean tumor sizes accompanied by expert opinion on the differences observed. To assess the *statistical significance* of treatment effectiveness, on the other hand, we calculated differences – for particular (available) time points (i.e. days) – between mean tumor sizes in the control groups and groups receiving mAb therapy as well as those between the latter groups and the groups treated with targeted polymers (e.g. mAb19 vs. mAb). For the daily time series of these differences, statistical hypothesis tests of linear trend slopes equality to zero were carried out. The Bonferroni correction was used to smooth the significance level for multiple simultaneous hypothesis tests.

Data was analyzed using the statistic calculation. Each model was covering different time periods with different numbers of known data points. For the purpose of assessing the statistical significance of treatment effectiveness, we made an assumption that the calculated differences (between mean tumor sizes in the control groups and groups receiving mAb therapy as well as those between the latter groups and the groups treated with targeted polymers) were generated by a process which includes a deterministic linear trend in the form of.

$$y_t = \beta_0 + \beta_1 t + \varepsilon_t$$

where y_t denotes the data-generating stochastic process of the analyzed differences, $t = 1, 2, \ldots T$ is a time variable, T signifies the length of the experiment (not the same for all experiments) in days and β_t is the Gaussian IID white noise. Having concurrently performed 15 statistical hypothesis tests about the zero value of β_1, the Bonferroni correction of 10% and 1% simultaneous significance levels was utilized, resulting in individual significance levels of 0.6667% and 0.0667%, respectively. The results are shown in Table 4.

3. Results and discussion

We have recently shown that one-point attachment of synthetic polymer precursors to the mAb leads to a highly defined APDC suitable for the treatment of various malignancies [25,46]. Here, we focused on the therapeutic potential of stimuli-sensitive actively targeted biomaterials composed from central mAb decorated with biocompatible polymer chains carrying classic chemotherapeutic drug doxorubicin, see Scheme 1. We investigated in detail in vivo therapeutic potential of the prepared constructs targeted by various mAbs on a panel of three PDX lymphoma models derived from patients with aggressive B-NHL. Two PDX models were established from patients with treatment-refractory B-NHL, who failed after rituximab-based therapies. One PDX models was derived from a patient with so far untreated B-NHL and served as a positive control for anti-CD20-based approaches. Apart from widely tested CD19 targeting with two different CD19 antibodies we

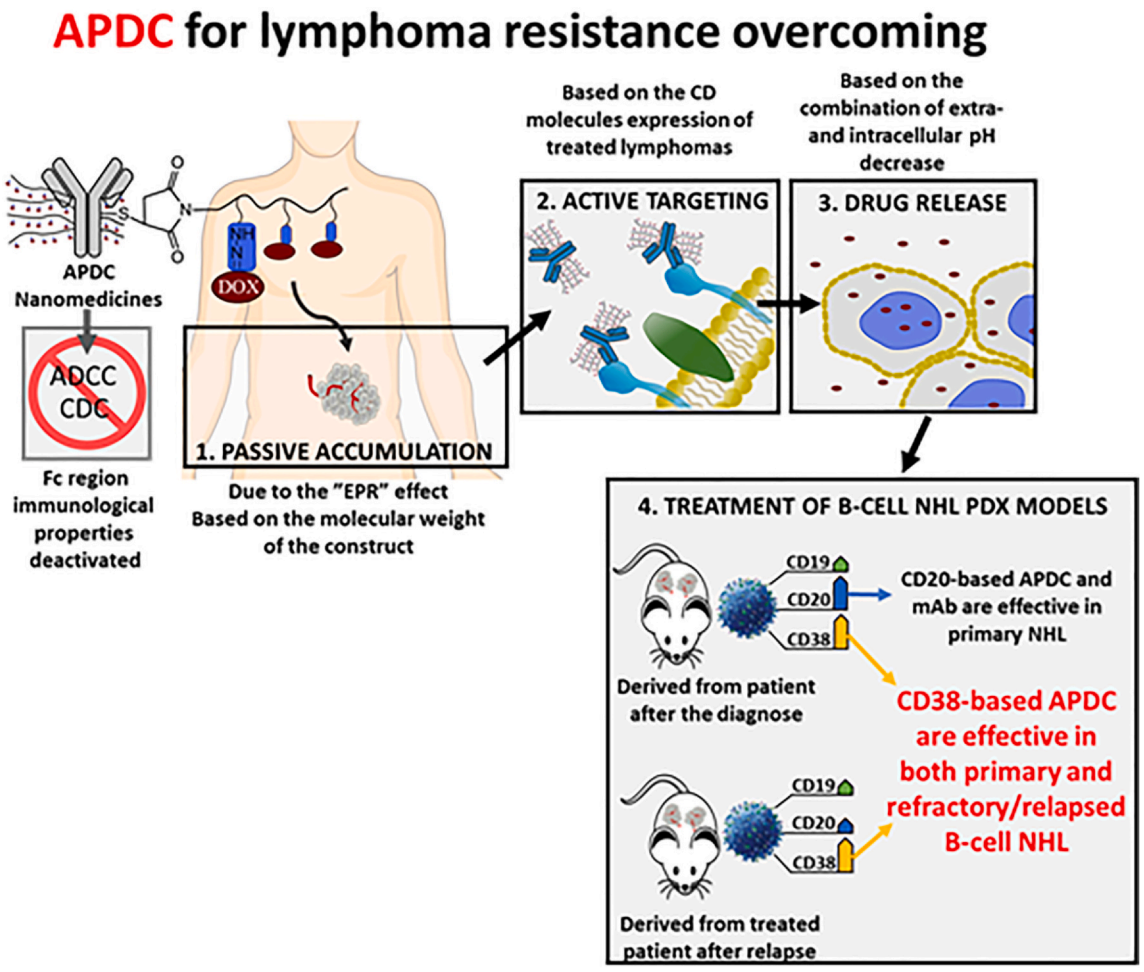

Scheme 1. Overall description of the mode of the action of designed and developed APDC.

also studied a potential of CD38-targeting with the commercially available therapeutic monoclonal antibody daratumumab. In addition to the fact that daratumumab is approved for the therapy of multiple myeloma, our recent pivotal data suggest the downregulation of CD38 antigen (plausibly by internalization of the antibody-antigen complexes) upon treatment of PDX bearing mice with the naked daratumumab antibody [47–49].

3.1. Synthesis of polymer precursors

Polymer precursors were prepared using the free radical polymerization initiated by TT functionalized azo-initiator to reproducibly prepare semitelechelic copolymer of HPMA and monomer with protected hydrazide groups (Fig. 1).

The polymerization was carried out to obtain the polymer precursor **P*** with molar mass under the renal threshold limit for HPMA-based polymers ~50–70,000 g/mol [50] so the polymer chains could be excluded from body by glomerular filtration after fulfilling their role in the organism and degradation of the whole APDC construct. In the second step, TT end groups were substituted with MI reactive groups and hydrazide protecting groups were removed to give polymer precursor **P** with similar physico-chemical properties to **P***. The functionality of maleimide functional groups decreased to the value close to 1 what fulfils the semitelechelic character of the polymer enabling the one point grafting of polymer precursor to the mAb. MI groups of polymer **P,** used as a control in ^{51}**Cr** release assay determining CDC and

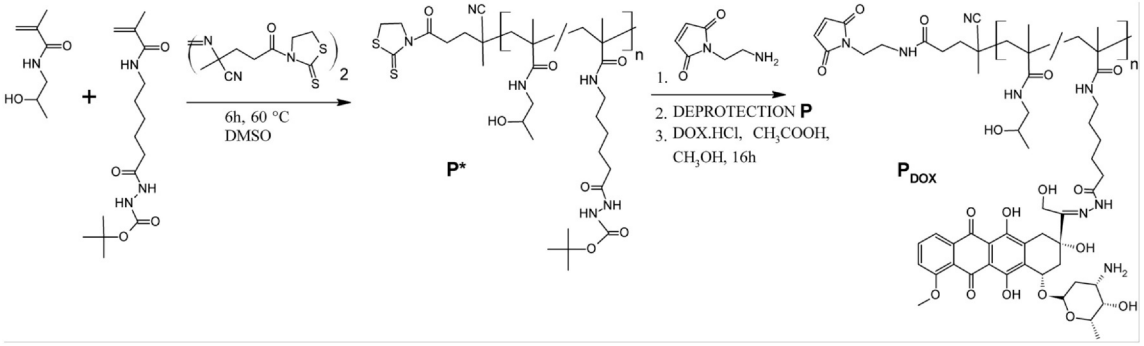

Fig. 1. Scheme of the synthesis of the semitelechelic HPMA based copolymer precursor containing hydrazone bound Dox - $\mathbf{P_{DOX}}$ and the maleimide terminal group.

ADCC, were modified with access of cysteine prior the experiment. Finally, anthracycline drug Dox was connected by hydrazone bond. Polymer precursor $\mathbf{P_{DOX}}$ contained 9.2 wt% of drug a sufficient amount for the follow-up synthetic and evaluation steps (Table 1). The higher molecular weight of the polymer precursor $\mathbf{P_{DOX}}$ could be ascribed partly to the inconsistency of M_w determination based on anthracyclines absorption spectrum which is partly overlapping with used laser in chromatography [51] and partly to the cross-reaction of maleimides with hydrazide groups or amino group presented in the structure of the doxorubicin. Nevertheless, the $\mathbf{P_{DOX}}$ had the M_w below the renal threshold and increased M_w could even enhance the time of circulation of the APDC. We can summarize that all the polymer precursors are useable for the further APDC synthesis.

3.2. APDC synthesis and characterization

Five comparable APDC were synthesized, see Table 2, using the same protocol employing "Michael addition". The free thiol groups of mAb, introduced by mild reduction using dithiothreitol, were reacted with main-chain end located maleimide group of the polymer precursors **P** or $\mathbf{P_{DOX}}$. Mild reduction of mAb led in all used mAb to formation of 8–12 thiol groups per mAb which was a sufficient amount of reactive groups for the conjugation reaction. As published elsewhere [34] and determined by GPC, electrophoresis and binding ability assay, the mild reduction of disulfide bridges does not influenced the overall structure and activity of mAb. Within the following click reaction, between sulfhydryl groups of reduced mAb and main-chain end MI groups of polymers, all APDC formed *star*-like structures employing the one point attachment strategy for linking several polymer chains to mAb, see Fig. 2. In sum, for all APDC we have not found any significance of the mAb degradation to fragments during the synthetic steps.

All APDC contained after the reaction approximately 45–50% of mAb in the conjugate. The molecular weight was comparable for all APDC, a small increase of the molecular weight for **mAb19-$\mathbf{P_{DOX}}$** and **mAb38-$\mathbf{P_{DOX}}$** could be escribed to the partial cross-linking of two mAb by polymer containing two MI functional groups. Nevertheless, the increase of molecular weight was very small and did not cause significant increase of dispersity. All APDC showed similar content of the drug (~ 5 wt%), which was sufficient for the following biological experiments. APDC contained after the reaction small content of unreacted polymer precursor, up to 12%. We suppose that the precursor would be eliminated from the body in a short time due to the renal filtration and would not affect the in vivo experiments. After the APDC construct formation the size in the solution of all there APDCs increase in comparison to free mAb, Rh ~ 5 nm, or polymer precursor, Rh = 4.2. The hydrodynamic radius of APDCs increased approximately two times in contrast to free mAb, thus showing the possibility for prolonged circulation of all formed APDCs leading to the much profound simultaneous passive and active targeting ability into the lymphomas.

Dispersity of all APDCs was below 1.5 thus showing their high uniformity. In the case of **mAb19B-$\mathbf{P_{DOX}}$**, **mAb20-P** and **mAb38-P** the dispersity dropped to 1.1 showing the potential of the method to synthesize the well-defined APDC. Unreacted thiol groups on mAb were blocked by adding the *N*-ethylmaleimide to avoid any possible cross-linking of the synthesized APDC. All the APDC showed proper physicochemical properties which nominate them as suitable candidates for further studies.

3.3. Drug release study

Stimuli sensitive nanomedicines should enable the drug activation upon the external stimuli from the target tissue or cells. Moreover, stability during the circulation is prerequisite for the elimination of desired effects of the treatment and increase the efficacy of the target tissue accumulation. Stability of prepared APDC containing pH-sensitive hydrazone bond in environment modelling blood stream (pH 7.4) and drug release kinetics from the polymer carriers at model of the extracellular tumor environment (pH 6.5) and of tumor cells (pH 5.0) were measured, see Fig. 3. All the APDC were highly stable in the PBS buffer (pH 7.4) mimicking the condition of the blood stream with up to 10–18% release of drug within one day. Similar results were obtained also in plasma proving the APDC stability after the injection and during the delivery to the lymphoma mass. On the other hand, fast drug release with 60–75% in 5 h in the buffer mimicking the intracellular condition of the tumor cells, pH 5.0, was observed and the pH-sensitive behavior of APDC was unambiguously validated. Indeed, even in the model of extracellular tumor environment, pH 6.5, accelerated drug release showing around 55–64% of drug released within 24 h was found. There were slight differences between the APDCs, which were not significant for the overall pH-responsiveness of APDCs. We can summarize that all

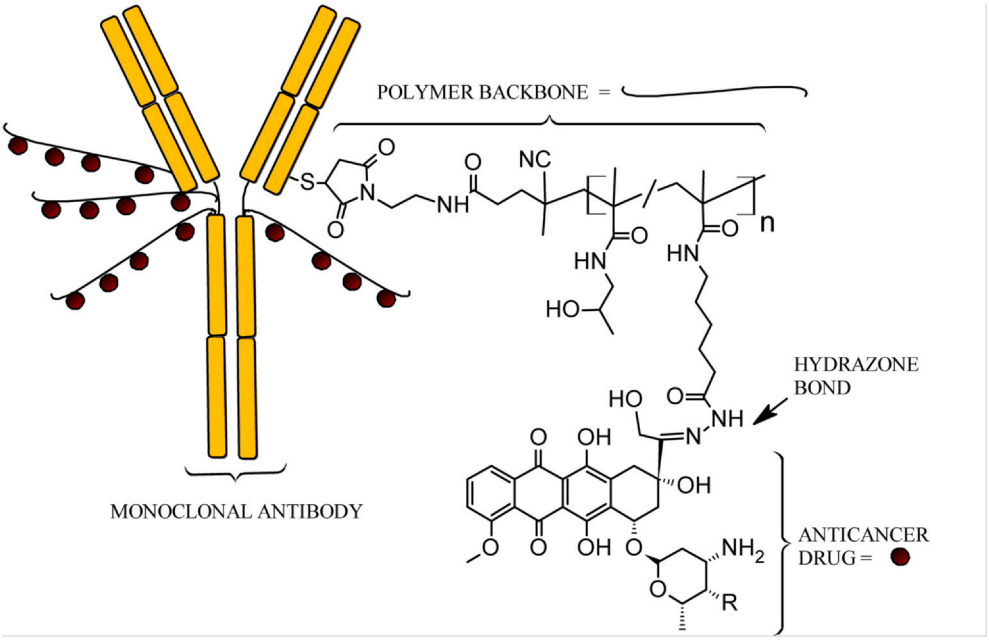

Fig. 2. Schematic description of APDC composed of the central targeting antibody decorated with polymer drug carriers with attached drug via hydrazone bond.

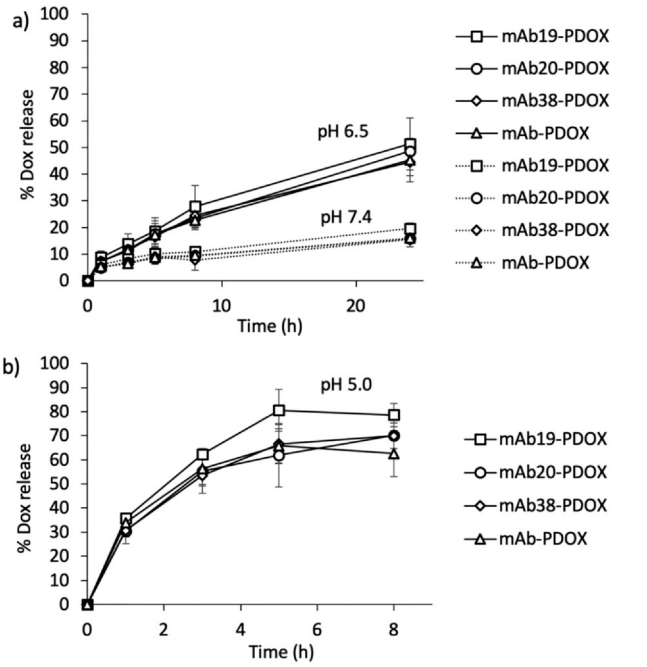

Fig. 3. Release of Dox from the conjugates **mAb19-P_{DOX}** (□), **mAb20-P_{DOX}** (○), **mAb38-P_{DOX}** (◊) and **mAb-P_{DOX}** (Δ) at 37 °C in various pH modelling blood stream condition – pH 7.4, dashed line in a); extracellular environment – pH 6.5, full line in a); and intracellular environment in lysosomes – pH 5.0, full line in b); $n = 3$.

the APDC have the same and highly favourable pH-sensitive release profile of the drug, highly valuable for the drug activation in hypoxic lymphoma tissue or lymphoma cells.

3.4. In vitro study of APDC binding efficiency

Grafting of the mAb structure with polymers has potential risk of affecting its effectiveness and binding ability to their targeting epitopes on cell membrane. Nevertheless, single-point attachment of the polymer precursor to the thiol groups of reduced antibody avoids the risk of modifying the hypervariable region of the antibody and it is most likely attached to the hinge area. To evaluate the possible decrease of binding ability, we evaluated in detail the binding efficiency of the prepared APDC to their antigens. The expression of CD19, CD20 and CD38 on UPF4D and SU-DHL-5 cell lines was evaluated using the flow cytometry (Figure SI1). UPF4D cell line showed the expression of all three CD molecules, while only CD19 and CD20 expression was found for SU-DHL-5 cell line. The binding efficacy of the **mAb19-P_{DOX}**, **mAb20-P_{DOX}** and **mAb38-P_{DOX}** were compared to the binding efficacy of original unmodified mAb mAb19, mAb20 and mAb38 using UPF4D and SU-DHL-5 B-cell lines, Fig. 4. To evaluate the binding efficacy precisely the experiment setup employing consequential binding of APC-labeled antibodies to the appropriate epitope blocked by APDC or mAb in the previous step was applied.

Any significant difference of binding activity was not detected for the UPF4D cell line between mAb19, mAb38 and their APDCc at concentration 100 and 10 μg/mL. Decrease of binding activity of **mAb19-P_{DOX}** and **mAb38-P_{DOX}** was observed only at the lowest concentration of 1 μg/mL. Indeed, significantly lower binding activity was observed for both cell lines in the case of **mAb20-P_{DOX}** at concentrations 10 and 1 μg/mL. Similarly as for UPF4D cell line the binding activity of **mAb19-P_{DOX}** for SU-DHL-5 cell line was not decreased at concentrations 100 and 10 μg/mL compared to mAb19. Again, the binding activity was significantly decreased only at the lowest concentration of **mAb19-P_{DOX}**. Measuring the efficiency for CD38 biding ability for SU-DHL-5 was not possible due to the lack of the CD38 epitopes. We can summarize that the binding ability of the prepared APDCs was found comparable with the original mAb in higher concentration tested, where the saturation of the CD epitopes on the cell should occur. Indeed, the binding ability was partially decreased and affected at lower concentration in the both cell lines UPF4D and SU-DHL-5, proving the influence of the modification of mAb into its binging ability. Nevertheless, even at low concentration all APDC tested were able to bind to the epitopes on the cells. We thus confirmed the ability of the conjugates, antibodies decorated with polymer, to recognize their targeting CD molecules and proved their binding to the cell surface with high efficiency comparable to the unmodified antibodies in their higher concentrations.

3.5. In vitro cytotoxicity

The in vitro cytotoxic activity of the conjugates **mAb19-P_{DOX}**, **mAb20-P_{DOX}**, **mAb38-P_{DOX}**, **mAb19B-P_{DOX}**, **Ab-P_{DOX}**, **P_{DOX}** and free DOX was measured using Alamar Blue proliferating assay. All mAb targeted constructs containing hydrazone bound Dox showed comparable cytotoxicity without significant differences. This could be ascribed to the release of the part of the drug already in the extracellular space during the experiment. Cytotoxic effect could be caused by both, the drug released inside the cell after the internalization of APDCs to the cells and also by Dox released from the APDCs in the extracellular space and penetrate throw the cell membrane independently on the APDC targeting abilities. SU-DHL-5 cell line showed higher sensitivity to the anthracycline drugs than UPF4D cell line. **P_{DOX}** alone showed lower toxicity on less sensitive UPF4D cell line in comparison to all mAb containing constructs, showing the mAb-triggered targeting benefit already in vitro. No significant difference in cytotoxicity was found between polymer alone and targeted systems on SU-DHL-5 cell line. We hypothesize that the higher effectivity of polymer alone is also connected with higher sensitivity of the SU-DHL-5 cell line to doxorubicin, which is partly released from all the pH-responsive APDCs in the medium within the 3 day experiment. All the APDCs containing specific monoclonal antibodies were more cytotoxic than the **Ab-P_{DOX}** containing nonspecific antibody, thus proving the benefit of the specific active targeting on cytotoxicity. Expectably, the toxicity of free Dox was significantly higher in contrast to all the polymer-based systems as was several times described previously. This phenomenon is based on the rapid internalization of free drug in comparison to the much slower process of endocytosis of polymer-based nanomedicines (Table 3).

3.6. CDC and ADCC determination

Due to the possible masking of the antibody Fc fragment after the modification with polymer chains in APDC and connected depletion of ADCC and/or CDC biological activity of mAb, we evaluated the ability of the developed APDC to induce ADCC or CDC using standard Cr-release assay. Two drug free analog APDC constructs, **mAb20-P** and **mAb38-P**, based on anti-CD20 and anti-CD38 mAb modified with polymer precursor **P** were synthesized. ADCC and CDC activity of these constructs was compared with the activity of unmodified mAb rituximab (anti-CD20) and daratumumab (anti-CD38) and their **mAb20-P** and **mAb38-P** constructs. Three cell lines were used for the Cr-release assay: RAJI cell line expressing both CD20 and CD38; SUDHL5 cell line expressing CD20, but not CD38; and UPF4D, which expresses CD38, but not CD20 (CD20-negative side-population was used for the Cr-release experiments). UPF4D was derived in parallel from the same patient as the PDX model VFN-D2 used for in vivo experiments (Fig. 5).

The Cr-release assays confirmed that the extent of the antibody-triggered cell lysis correlated with the level of expression of the targeted CD antigens. In addition, the functional assays confirmed the anticipated weakening or even abrogation of immune-mediated activities of the tested monoclonal antibodies after their conjugation to polymer

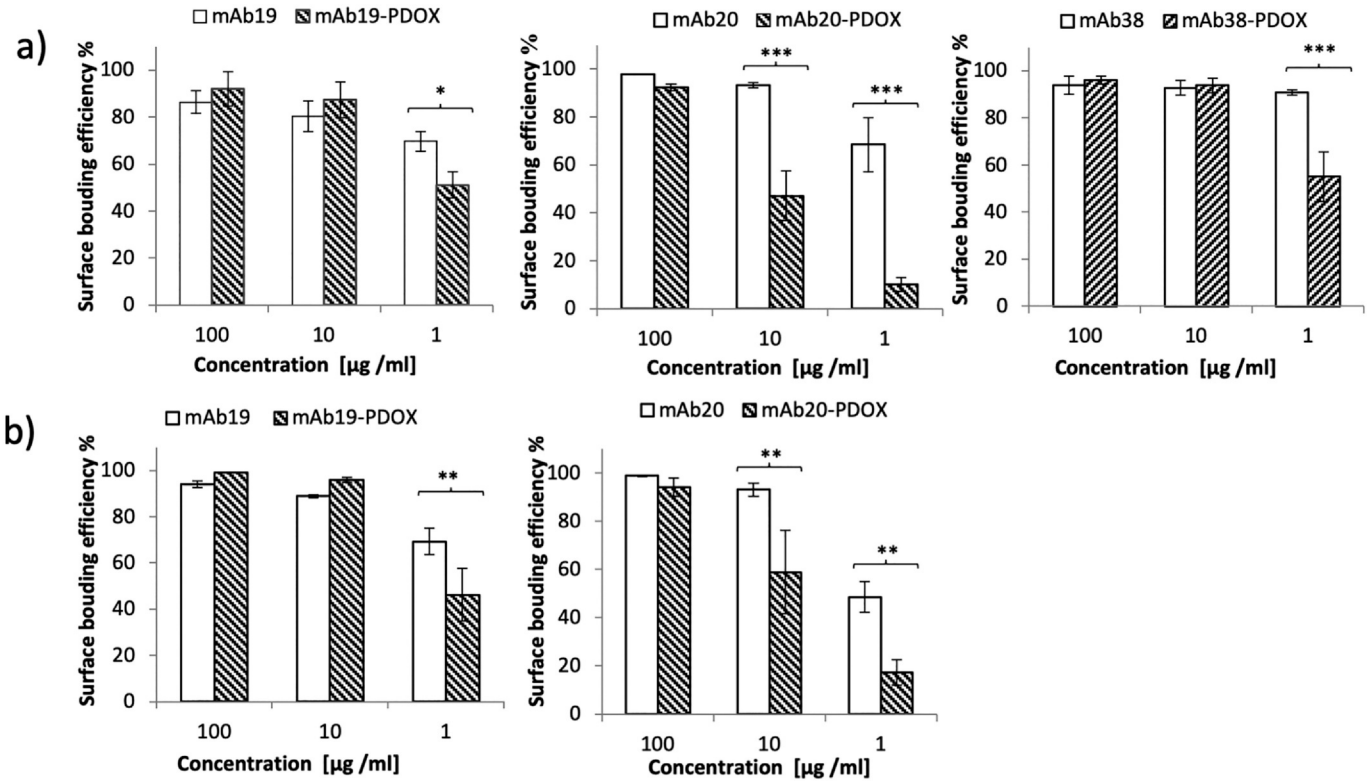

Fig. 4. Comparison of binding efficiency of APDC (**mAb19-P_{DOX}**, **mAb20-P_{DOX}**, **mAb38-P_{DOX}**) and original antibodies (mAb19, mAb20, mAb38) to the cell surface membrane epitopes. The binding activity was evaluated by flow cytometry for a) UPF4D and b) SU-DHL-5 cell lines. Significant differences are labeled with asterisks: ***$P < 0.001$, **$P < 0.01$, and *$P < 0.05$.

Table 3
Cytotoxicity expressed as IC_{50}.

Cell line APDC	UPF4D	SU-DHL-5
	IC_{50} (ng DOX eq./mL)	IC_{50} (ng DOX eq./mL)
mAb19-P_{DOX}	289 ± 27	95 ± 24
mAb19B-P_{DOX}	378 ± 161	84 ± 47
mAb20-P_{DOX}	262 ± 24	82 ± 23
mAb38-P_{DOX}	276 ± 63	89 ± 37
Ab-P_{DOX}	453 ± 53	221 ± 69
P_{DOX}	1041 ± 441	107 ± 86
DOX	16 ± 4	3.5 ± 1.7

chains. In summary, the modification of the mAb by several polymer chains, using the orthogonal one-point maleimide–thiol coupling in the hinge area of mAb, are most probably blocking sterically the structures of the Fc fragments which are responsible for activating the CDC or ADCC. The results suggest that the APDC constructs induce cell cytotoxicity mainly due to the genotoxic effect of the carried drug, i.e. doxorubicin. In this case, the antibodies serve mainly as the targeting moieties with largely suppressed immunological mode-of-action.

3.7. In vivo anti-lymphoma activity on a panel of PDX lymphoma models

In vivo experiments were implemented on three PDX models derived from two patients after failure of CD20-based front-line therapies (VFN-D2, VFN-B2) and one so far untreated patient (VFN-M5), see

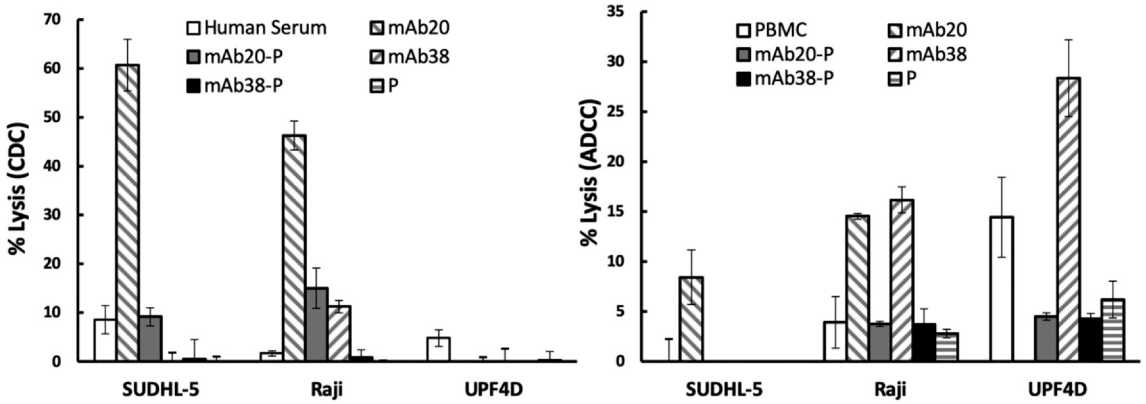

Fig. 5. Evaluation of cell lysis (%) due to the CDC or ADCC using Cr release assay. Comparison of the polymer-modified antibodies **mAb20-P**, **mAb38-P**, polymer **P** (concentration 20 µg/mL, in polymer-modified antibodies equal to 10 µg/mL) and unmodified antibodies **mAb20** and **mAb38** (concentration 10 µg/mL) normalized to the Isotype control, cell lines SUDHL-5, Raji and UPF4D, $n = 3$.

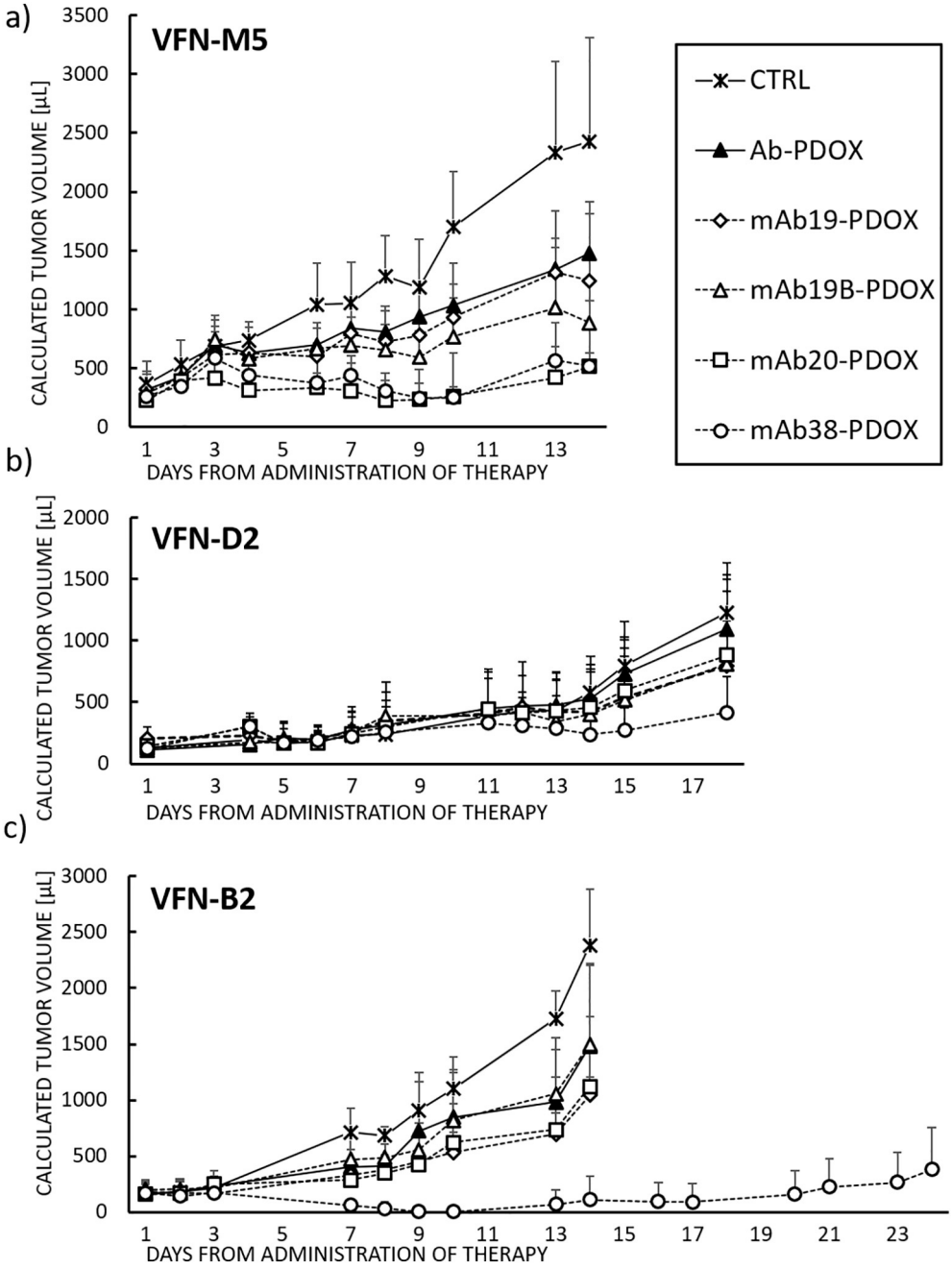

Fig. 6. In vivo activity of the APDC after administration single dose of the conjugates **mAb19-P$_{DOX}$**, **mAb19B-P$_{DOX}$**, **mAb20-P$_{DOX}$**, **mAb38-P$_{DOX}$**, **Ab-P$_{DOX}$** compared to the untreated control CTRL and the comparison of the tumor size after the autopsy done on three PDX models a) VFN-M5; b) VFN-D2; c) VFN-B2. VFN-B2 $n = 6$, WFN-M5 $n = 7$, WFN-D2 $n = 7$.

Table 4
Statistical analysis of in vivo efficacy.

Differences	VFN-M5	VFN-D2	VFN-B2
CTRL vs. Ab-P$_{DOX}$	0.0000***	0.1565	0.0007*
Ab-P$_{DOX}$ vs. mAb19-P$_{DOX}$	0.0313	0.0001***	0.0014*
Ab-P$_{DOX}$ vs. mAb19B-P$_{DOX}$	0.0001***	0.0003***	0.9523
Ab-P$_{DOX}$ vs. mAb20-P$_{DOX}$	0.0000***	0.0019*	0.0008*
Ab-P$_{DOX}$ vs. mAb38-P$_{DOX}$	0.0000***	0.0001***	0.0000***

P-values of partial *t*-tests about zero slope of mean tumor size differences (statistical significance: * 10% and *** 1% simultaneous significance level).

characterization in the SI. The anti-lymphoma efficacy of APDCs was compared using single low dose, 5 mg/kg Dox equivalent. The treatment was neither accompanied by signs of apparent toxicity, nor did it impact weight of the experimental animals. The overall good tolerance of the single injection-based therapy suggests potential for future dose escalation with better anti-lymphoma efficacy.

The in vivo data confirmed that APDCs targeted with mAbs (**mAb19-P$_{DOX}$**, **mAb19B-P$_{DOX}$**, **mAb20-P$_{DOX}$** and **mAb38-P$_{DOX}$**) were significantly more efficient in suppressing lymphoma growth than non-specific APDC (**Ab-P$_{DOX}$**) (Fig. 6, Table 4). The partial effect of non-specific APDC could be ascribed to the EPR effect-based accumulation of the non-targeted nanotherapeutics. Anti-lymphoma activity of CD20- and CD38-targeting APDCs was comparable in mice xenografted with VFN-M5 PDX cells derived from so far untreated patient. In contrast,

treatment of mice xenografted with PDX cells derived from patients, who failed after rituximab-based regimen (VFN-D2, VFN-B2) confirmed significantly better anti-lymphoma efficacy of the APDC targeted with anti-CD38 daratumumab compared to anti-CD20 rituximab and other APDCs. Even with small single Dox eq. dose the anti-CD38 APDC induced long-term control of growth of. The reason for the observed lower efficacy of the tested conjugates targeted with CD19 mAbs remains elusive and will be further studied.

Because we have previously demonstrated marked weakening of immunological activities of the mAbs in APDCs, the efficacy of the conjugates targeted with mAbs is predominantly a consequence of targeted delivery of doxorubicin to the tumor tissue. This is particularly important, because despite promising preclinical data, a recently published study with single-agent daratumumab in patients with relapsed/refractory DLBCL was prematurely terminated due to low anti-tumor efficacy of the naked anti-CD38 antibody [52,53]. In contrast, CD38-based APDC can offer an effective alternative based on different anti-lymphoma mode of action, Scheme 1, as already mentioned by Weinstein [54]. Historically, we have witnessed similar difference in anti-lymphoma efficacy between a naked anti-CD30 antibody SGN-30 (negligible) and CD30-based ADC brentuximab-vedotin (substantial) [55,56].

4. Conclusion

In this proof-of-concept study we confirmed that active targeting of APDCs with selected mAbs can significantly enhance their anti-lymphoma efficacy compared to the nontargeted nanoterapeutics. Moreover, stimuli sensitive behavior made the developed APDCs good candidates for highly effective therapy of R/R lymphomas with limited side effects. From the tested cell surface antigens, targeting of CD38 with commercially available mAb daratumumab appears particularly promising, especially in the subgroup of patients with relapsed, CD38-positive B-NHL, with decreased or absent CD20 expression due to previous rituximab-based therapies. We demonstrated that the anti-lymphoma efficacy of the tested APDCs is mediated largely by targeted delivery of doxorubicin to the lymphoma with limited immunologic mode-of-action. The results represent a new algorithm of personalized anti-tumor therapy based on highly innovative actively targeted drug-delivery biomaterials.

Acknowledgement

This work was supported by the project “BIOCEV – Biotechnology and Biomedicine Centre of the Academy of Sciences and Charles University” (CZ.1.05/1.1.00/02.0109), from the European Regional Development Fund, by the Ministry of Education, Youth and Sports of CR within the National Sustainability Program II, Project Biocev-Far LQ1604, Ministry of Education, Youth and Sports of the Czech Republic Institutional Support PROGRES Q26/LF1 and PROGRES Q28/LF1, Charles University Grant Agency Research Grant GA-UK 250421, Charles University Center of Excellence UNCE/MED/016, and by the Czech Science Foundation projects No, 19-01417S.

Appendix A. Supplementary data

Supplementary data to this article can be found online at https://doi.org/10.1016/j.jconrel.2020.08.042.

References

[1] J.O. Armitage, R.D. Gascoyne, M.A. Lunning, F. Cavalli, Non-Hodgkin lymphoma, Lancet 390 (2017) 298–310, https://doi.org/10.1016/S0140-6736(16)32407-2.
[2] S.H. Swerdlow, E. Campo, S.A. Pileri, N.L. Harris, H. Stein, R. Siebert, R. Advani, M. Ghielmini, G.A. Salles, A.D. Zelenetz, E.S. Jaffe, 2016 WHO classification of lymphoid neoplasms, Blood J. 127 (2017) 453–462, https://doi.org/10.1182/blood-2016-01-643569.The.
[3] B. Coiffier, E. Lepage, J. Brière, R. Herbrecht, H. Tilly, R. Bouabdallah, P. Morel, E. Van Den Neste, G. Salles, P. Gaulard, F. Reyes, C. Gisselbrecht, CHOP chemotherapy plus rituximab compared with CHOP alone in elderly patients with diffuse large-B-cell lymphoma, N. Engl. J. Med. 346 (2002) 235–242.
[4] G.M. Keating, Rituximab: a review of its use in chronic lymphocytic leukaemia, low-grade or follicular lymphoma and diffuse large B-cell lymphoma, Drugs. 70 (2010) 1445–1476, https://doi.org/10.2165/11201110-000000000-00000.
[5] S.M. Ansell, Non-Hodgkin lymphoma: diagnosis and treatment, Mayo Clin. Proc. 90 (2015) 1152–1163, https://doi.org/10.1016/j.mayocp.2015.04.025.
[6] P. Feugier, A. Van Hoof, C. Sebban, P. Solal-Celigny, R. Bouabdallah, C. Fermé, B. Christian, E. Lepage, H. Tilly, F. Morschhauser, P. Gaulard, G. Salles, A. Bosly, C. Gisselbrecht, F. Reyes, B. Coiffier, Long-term results of the R-CHOP study in the treatment of elderly patients with diffuse large B-cell lymphoma: a study by the groupe d'etude des lymphomes de l'adulte, J. Clin. Oncol. 23 (2005) 4117–4126, https://doi.org/10.1200/JCO.2005.09.131.
[7] M.R. Smith, Rituximab (monoclonal anti-CD20 antibody): mechanisms of action and resistance, Oncogene. 22 (2003) 7359–7368, https://doi.org/10.1038/sj.onc.1206939.
[8] M. Crump, S.S. Neelapu, U. Farooq, E. Van Den Neste, J. Kuruvilla, J. Westin, B.K. Link, A. Hay, J.R. Cerhan, L. Zhu, S. Boussetta, L. Feng, M.J. Maurer, L. Navale, J. Wiezorek, W.Y. Go, C. Gisselbrecht, Outcomes in refractory diffuse large B-cell lymphoma: results from the international SCHOLAR-1 study, Blood. 130 (2017) 1800–1808, https://doi.org/10.1182/blood-2017-03-769620.
[9] C. Gisselbrecht, E. Van Den Neste, How I manage patients with relapsed/refractory diffuse large B cell lymphoma, Br. J. Haematol. 182 (2018) 633–643, https://doi.org/10.1111/bjh.15412.
[10] E. Van Den Neste, N. Schmitz, N. Mounier, D. Gill, D. Linch, M. Trneny, N. Milpied, J. Radford, N. Ketterer, O. Shpilberg, U. Dührsen, D. Ma, J. Brière, C. Thieblemont, G. Salles, C.H. Moskowitz, B. Glass, C. Gisselbrecht, Outcome of patients with relapsed diffuse large B-cell lymphoma who fail second-line salvage regimens in the international CORAL study, Bone Marrow Transplant. 51 (2016) 51–57, https://doi.org/10.1038/bmt.2015.213.
[11] T.A. Davis, D.K. Czerwinski, R. Levy, Therapy of B-cell lymphoma with anti-CD20 antibodies can result in the loss of CD20 antigen expression, Clin. Cancer Res. 5 (1999) 611–615.
[12] Z.N. Soe, D. Allsup, The use of ofatumumab in the treatment of B-cell malignancies, Future Oncol. 13 (2017) 2611–2628, https://doi.org/10.2217/fon-2017-0275.
[13] D. Jovanovic, P. Djurdjevic, N. Andjelkovic, L. Zivic, Possible role of CD22, CD79b and CD20 expression in distinguishing small lymphocytic lymphoma from chronic lymphocytic leukemia, Contemp. Oncol. 18 (1) (2014) 29–33, https://doi.org/10.5114/wo.2013.38570.
[14] R.H. Advani, D. Lebovic, A. Chen, M. Brunvand, A. Goy, J.E. Chang, E. Hochberg, S. Yalamanchili, R. Kahn, D. Lu, P. Agarwal, R.C. Dere, H.J. Hsieh, S. Jones, Y.W. Chu, B.D. Cheson, Phase i study of the anti-CD22 antibody-drug conjugate pinatuzumab vedotin with/without rituximab in patients with relapsed/refractory B-cell non-hodgkin lymphoma, Clin. Cancer Res. 23 (2017) 1167–1176, https://doi.org/10.1158/1078-0432.CCR-16-0772.
[15] E.D. Deeks, Polatuzumab Vedotin: First Global Approval, Drugs 79 (2019) 1467–1475, https://doi.org/10.1007/s40265-019-01175-0.
[16] M.C.A. Palanca-Wessels, M. Czuczman, G. Salles, S. Assouline, L.H. Sehn, I. Flinn, M.R. Patel, R. Sangha, A. Hagenbeek, R. Advani, H. Tilly, O. Casasnovas, O.W. Press, S. Yalamanchili, R. Kahn, R.C. Dere, D. Lu, S. Jones, C. Jones, Y.W. Chu, F. Morschhauser, Safety and activity of the anti-CD79B antibody-drug conjugate polatuzumab vedotin in relapsed or refractory B-cell non-Hodgkin lymphoma and chronic lymphocytic leukaemia: A phase 1 study, Lancet Oncol. 16 (2015) 704–715, https://doi.org/10.1016/S1470-2045(15)70128-2.
[17] H. Maeda, H. Nakamura, J. Fang, The EPR effect for macromolecular drug delivery to solid tumors: improvement of tumor uptake, lowering of systemic toxicity, and distinct tumor imaging in vivo, Adv. Drug Deliv. Rev. 65 (2013) 71–79, https://doi.org/10.1016/j.addr.2012.10.002.
[18] N. Bertrand, J. Wu, X. Xu, N. Kamaly, O.C. Farokhzad, Cancer nanotechnology: the impact of passive and active targeting in the era of modern cancer biology, Adv. Drug Deliv. Rev. 66 (2014) 2–25, https://doi.org/10.1016/j.addr.2013.11.009.
[19] F. Danhier, O. Feron, V. Préat, To exploit the tumor microenvironment: passive and active tumor targeting of nanocarriers for anti-cancer drug delivery, J. Control. Release 148 (2010) 135–146, https://doi.org/10.1016/j.jconrel.2010.08.027.
[20] L. Zhang, Y. Fang, J. Kopeček, J. Yang, A new construct of antibody-drug conjugates for treatment of B-cell non-Hodgkin's lymphomas, Eur. J. Pharm. Sci. 103 (2017) 36–46, https://doi.org/10.1016/j.ejps.2017.02.034.
[21] O. Boutureira, J.L. Bernardes, Advances in Chemical Protein Modification, (2015), https://doi.org/10.1021/cr500399p.
[22] P. Dennler, E. Fischer, R. Schibli, Antibody conjugates: from heterogeneous populations to defined reagents, Antibodies. 4 (2015) 197–224, https://doi.org/10.3390/antib4030197.
[23] J.M.J.M. Ravasco, H. Faustino, A. Trindade, P.M.P. Gois, Bioconjugation with Maleimides: a useful tool for chemical biology, Chem. - A Eur. J. 25 (2019) 43–59, https://doi.org/10.1002/chem.201803174.
[24] A. Beck, L. Goetsch, C. Dumontet, N. Corvaïa, Strategies and challenges for the next generation of antibody–drug conjugates, Nat. Publ. Gr. (2017), https://doi.org/10.1038/nrd.2016.268.
[25] O. Lidický, O. Janoušková, J. Strohalm, M. Alam, P. Klener, T. Etrych, Anti-lymphoma efficacy comparison of anti-CD20 monoclonal antibody-targeted and non-targeted star-shaped polymer-prodrug conjugates, Molecules 20 (2015), https://doi.org/10.3390/molecules201119664.
[26] S.J. Sonawane, R.S. Kalhapure, T. Govender, Hydrazone linkages in pH responsive drug delivery systems, Eur. J. Pharm. Sci. 99 (2017) 45–65, https://doi.org/10.

1016/j.ejps.2016.12.011.
[27] K. Ulbrich, T. Etrych, P. Chytil, M. Jelínková, B. Říhová, HPMA copolymers with pH-controlled release of doxorubicin: in vitro cytotoxicity and in vivo antitumor activity, J. Control. Release 87 (2003) 33–47, https://doi.org/10.1016/S0168-3659(02)00348-6.
[28] Y.W. Chu, A. Polson, Antibody-drug conjugates for the treatment of B-cell non-Hodgkin's lymphoma and leukemia, Future Oncol. 9 (2013) 355–368, https://doi.org/10.2217/fon.12.189.
[29] B. Říhová, P. Kopečková, J. Strohalm, P. Rossmann, V. Větvička, J. Kopeček, Antibody-directed affinity therapy applied to the immune system: in vivo effectiveness and limited toxicity of daunomycin conjugated to HPMA copolymers and targeting antibody, Clin. Immunol. Immunopathol. 46 (1988) 100–114, https://doi.org/10.1016/0090-1229(88)90010-4.
[30] H. Dozono, S. Yanazume, H. Nakamura, T. Etrych, P. Chytil, K. Ulbrich, J. Fang, T. Arimura, T. Douchi, H. Kobayashi, M. Ikoma, H. Maeda, HPMA copolymer-conjugated Pirarubicin in multimodal treatment of a patient with stage IV prostate Cancer and extensive lung and bone metastases, Target. Oncol. 11 (2016) 101–106, https://doi.org/10.1007/s11523-015-0379-4.
[31] V. Šubr, Č. Koňák, R. Laga, K. Ulbrich, Coating of DNA/poly(L-lysine) complexes by covalent attachment of poly[N-(2-hydroxypropyl)methacrylamide], Biomacromolecules. 7 (2006) 122–130, https://doi.org/10.1021/bm050524x.
[32] K. Ulbrich, V. Šubr, J. Strohalm, D. Plocová, M. Jelínková, B. Říhová, Polymeric drugs based on conjugates of synthetic and natural macromolecules. I. Synthesis and physico-chemical characterisation, J. Control. Release 64 (2000) 63–79, https://doi.org/10.1016/S0168-3659(99)00141-8.
[33] M. Hruby, K. Ulbrich, Polymeric micellar pH-sensitive drug delivery system for doxorubicin, 103 (2005), pp. 137–148, https://doi.org/10.1016/j.jconrel.2004.11.017.
[34] O. Lidicky, O. Janouskova, J. Strohalm, M. Alam, P. Klener, T. Etrych, Anti-Lymphoma Efficacy Comparison of Anti-CD20 Monoclonal Antibody-Targeted and Non-Targeted Star-Shaped Polymer-Prodrug Conjugates, (2015), pp. 19849–19864, https://doi.org/10.3390/molecules201119664.
[35] T. Etrych, T. Mrkvan, B. Říhová, K. Ulbrich, Star-shaped immunoglobulin-containing HPMA-based conjugates with doxorubicin for cancer therapy, J. Control. Release 122 (2007) 31–38, https://doi.org/10.1016/j.jconrel.2007.06.007.
[36] V. Subr, L. Kostka, T. Selby-Milic, K. Fisher, K. Ulbrich, L.W. Seymour, R.C. Carlisle, Coating of adenovirus type 5 with polymers containing quaternary amines prevents binding to blood components, J. Control. Release 135 (2009) 152–158, https://doi.org/10.1016/j.jconrel.2008.12.009.
[37] T. Etrych, J. Strohalm, L. Kovář, M. Kabešová, B. Říhová, K. Ulbrich, HPMA copolymer conjugates with reduced anti-CD20 antibody for cell-specific drug targeting. I. Synthesis and in vitro evaluation of binding efficacy and cytostatic activity, J. Control. Release 140 (2009) 18–26, https://doi.org/10.1016/j.jconrel.2009.07.011.
[38] K. Ulbrich, T. Etrych, P. Chytil, M. Jelínková, B. Říhová, Antibody-targeted polymer-doxorubicin conjugates with pH-controlled activation, J. Drug Target. 12 (2004) 477–489, https://doi.org/10.1080/10611860400011869.
[39] T. Etrych, M. Jelínková, B. Říhová, K. Ulbrich, New HPMA copolymers containing doxorubicin bound via pH-sensitive linkage: synthesis and preliminary in vitro and in vivo biological properties, J. Control. Release 73 (2001) 89–102, https://doi.org/10.1016/S0168-3659(01)00281-4.
[40] T. Etrych, P. Chytil, M. Jelínková, B. Říhová, K. Ulbrich, Synthesis of HPMA copolymers containing doxorubicin bound via a hydrazone linkage. Effect of spacer on drug release and in vitro cytotoxicity, Macromol. Biosci. 2 (2002) 43–52, https://doi.org/10.1002/1616-5195(20020101)2:1<43::AID-MABI43>3.0.CO;2-8.
[41] V. Subr, J. Strohalm, K. Ulbrich, R. Duncan, I.C. Hume, Polymers containing enzymatically degradable bonds, XII. Effect of spacer structure on the rate of release of daunomycin and adriamycin from poly [N-(2-hydroxypropyl)-methacrylamide] copolymer drag carriers in vitro and antitumour activity measured in viv, J. Control. Release 18 (1992) 123–132, https://doi.org/10.1016/0168-3659(92)90181-P.
[42] G.L. Ellman, Tissue sulfhydryl groups, Arch. Biochem. Biophys. 82 (1959) 70–77, https://doi.org/10.1016/0003-9861(59)90090-6.
[43] E.A. Brem, K. Thudium, S. Khubchandani, P.C. Tsai, S.H. Olejniczak, S. Bhat, W. Riaz, J. Gu, A. Iqbal, R. Campagna, J. Knight, C. Mavis, P. Hoskin, G. Deeb, J.F. Gibbs, G. Fetterly, M.S. Czuczman, F.J. Hernandez-Ilizaliturri, Distinct cellular and therapeutic effects of obatoclax in rituximab-sensitive and -resistant lymphomas, Br. J. Haematol. 153 (2011) 599–611, https://doi.org/10.1111/j.1365-2141.2011.08669.x.
[44] F. Pavanello, E. Zucca, M. Ghielmini, Rituximab: 13 open questions after 20 years of clinical use, Cancer Treat. Rev. 53 (2017) 38–46, https://doi.org/10.1016/j.ctrv.2016.11.015.
[45] L. Zou, G. Song, S. Gu, L. Kong, S. Sun, L. Yang, W.C. Cho, Mechanism and treatment of rituximab resistance in diffuse large Bcell lymphoma, Curr. Cancer Drug Targets 19 (2019) 681–687, https://doi.org/10.2174/1568009619666190126125251.
[46] T. Etrych, P. Chytil, L. Kovář, B. Říhová, K. Ulbrich, Micellar and Antibody-Targeted Polymer Therapeutics, Macromol. Symp. 295 (2010) 1–12, https://doi.org/10.1002/masy.200900066.
[47] E.N. Chini, C.C.S. Chini, J.M. Espindola Netto, G.C. de Oliveira, W. van Schooten, The pharmacology of CD38/NADase: an emerging target in Cancer and diseases of aging, Trends Pharmacol. Sci. 39 (2018) 424–436, https://doi.org/10.1016/j.tips.2018.02.001.
[48] K.A. Frerichs, N.A. Nagy, P.L. Lindenbergh, P. Bosman, J. Marin Soto, M. Broekmans, R.W.J. Groen, M. Themeli, L. Nieuwenhuis, C. Stege, I.S. Nijhof, T. Mutis, S. Zweegman, H.M. Lokhorst, N.W.C.J. van de Donk, CD38-targeting antibodies in multiple myeloma: mechanisms of action and clinical experience, Expert. Rev. Clin. Immunol. 14 (2018) 197–206, https://doi.org/10.1080/1744666X.2018.1443809.
[49] P. Vockova, M. Svaton, J. Karolova, E. Pokorna, M. Vokurka, P. Klener, Therapy with daratumumab for relapsed/refractory CD20-negative diffuse large B-cell lymphoma, Folia Biol. 66 (1) (2020) 17–23.
[50] T. Etrych, V. Šubr, J. Strohalm, M. Šírová, B. Říhová, K. Ulbrich, HPMA copolymer-doxorubicin conjugates: the effects of molecular weight and architecture on biodistribution and in vivo activity, J. Control. Release 164 (2012) 346–354, https://doi.org/10.1016/j.jconrel.2012.06.029.
[51] T. Etrych, T. Mrkvan, P. Chytil, Č. Koňák, B. Říhová, K. Ulbrich, N-(2-Hydroxypropyl)methacrylamide-based polymer conjugates with ph-controlled activation of doxorubicin. I. New synthesis, physicochemical characterization and preliminary biological evaluation, J. Appl. Polym. Sci. 109 (2008) 3050–3061.
[52] A. Vidal-Crespo, A. Matas-Céspedes, V. Rodriguez, C. Rossi, J.G. Valero, N. Serrat, A. Sanjuan Pla, P. Menéndez, G. Roué, A. López-Guillermo, E. Giné, E. Campo, D. Colomer, C. Bezombes, J. Lammerts van Bueren, C. Chiu, P. Doshi, P. Pérez-Galán, Daratumumab displays in vitro and in vivo anti-tumor activity in models of B cell non-Hodgkin lymphoma and improves responses to standard chemo-immunotherapy regimens, Haematologica (2019), https://doi.org/10.3324/haematol.2018.211904 haematol.2018.211904.
[53] G. Salles, A.K. Gopal, M.C. Minnema, K. Wakamiya, H. Feng, J.M. Schecter, M. Wang, Phase 2 study of daratumumab in relapsed/refractory mantle-cell lymphoma, diffuse large B-cell lymphoma, and follicular lymphoma, Clin. Lymphoma, Myeloma Leuk. 19 (2019) 275–284, https://doi.org/10.1016/j.clml.2018.12.013.
[54] S. Weinstein, I.A. Toker, R. Emmanuel, S. Ramishetti, I. Hazan-Halevy, D. Rosenblum, M. Goldsmith, A. Abraham, O. Benjamini, O. Bairey, P. Raanani, A. Nagler, J. Lieberman, D. Peer, Harnessing RNAi-based nanomedicines for therapeutic gene silencing in B-cell malignancies, Proc. Natl. Acad. Sci. U. S. A. 113 (2016) E16–E22, https://doi.org/10.1073/pnas.1519273113.
[55] A. Forero-Torres, J.P. Leonard, A. Younes, J.D. Rosenblatt, P. Brice, N.L. Bartlett, A. Bosly, L. Pinter-Brown, D. Kennedy, E.L. Sievers, A.K. Gopal, A phase II study of SGN-30 (anti-CD30 mAb) in Hodgkin lymphoma or systemic anaplastic large cell lymphoma, Br. J. Haematol. 146 (2009) 171–179, https://doi.org/10.1111/j.1365-2141.2009.07740.x.
[56] S. Horwitz, O.A. O'Connor, B. Pro, T. Illidge, M. Fanale, R. Advani, N.L. Bartlett, J.H. Christensen, F. Morschhauser, E. Domingo-Domenech, G. Rossi, W.S. Kim, T. Feldman, A. Lennard, D. Belada, Á. Illés, K. Tobinai, K. Tsukasaki, S.P. Yeh, A. Shustov, A. Hüttmann, K.J. Savage, S. Yuen, S. Iyer, P.L. Zinzani, Z. Hua, M. Little, S. Rao, J. Woolery, T. Manley, L. Trümper, D. Aboulafia, O. Alpdogan, K. Ando, L. Arcaini, L. Baldini, N. Bellam, N. Bartlett, D. Ben Yehuda, F. Benedetti, P. Borchman, D. Bordessoule, P. Brice, J. Briones, D. Caballero, A.M. Carella, H. Chang, J.W. Cheong, S.G. Cho, I. Choi, S. Choquet, A. Colita, A.G. Congui, F. D'amore, N. Dang, K. Davison, S. de Guibert, P. Brown, V. Delwail, J. Demeter, F. di Raimondo, Y.R. Do, E. Domingo, M. Douvas, M. Dreyling, T. Ernst, K. Fay, S.F. Ferrero, I.W. Flinn, A. Forero-Torres, C. Fox, J. Friedberg, N. Fukuhara, J. Garcia-Marco, J.G. Cruz, J.G. Codina, R. Gressin, A. Grigg, R. Gurion, C. Haioun, R. Hajek, M. Hanel, K. Hatake, R. Hensen, N. Horowitz, A. Huttmann, A. Illes, K. Ishizawa, M. Islas-Ohlmayer, E. Jacobsen, M. Janakiram, W. Jurczak, M. Kaminski, K. Kato, I. Kirgner, C.Y. Kuo, M.C. Lazaroiu, K. Le Du, J.S. Lee, S. LeGouill, P. LaRosee, I. Levi, B. Link, H. Maisonneuve, D. Maruyama, J. Mayer, J. McCarty, P. McKay, Y. Minami, H. Mocikova, E. Morra, J. Munoz, H. Nagai, O. O'Connor, S. Opat, R. Pettengell, A. Pezzutto, M. Pfreundschuh, A. Pluta, P.L. Porcu, H. Quach, A. Rambaldi, W. Renwick, R. Reyes, A.R. Izquierdo, J. Ruan, C. Rusconi, G. Salles, A. Santoro, J. Sarriera, H. Shibayama, C. Suh, A. Sureda, M. Tanimoto, M. Taniwaki, H. Tilly, M. Trneny, L. Trumper, N. Tsukamoto, U. Vitolo, J. Walewski, E. Weidmann, M. Wilhelm, M. Witzens-Harig, A. Yacoub, K. Yamamoto, S.S. Yoon, H.J. Yun, J. Zain, Brentuximab vedotin with chemotherapy for CD30-positive peripheral T-cell lymphoma (ECHELON-2): a global, double-blind, randomised, phase 3 trial, Lancet 393 (2019) 229–240, https://doi.org/10.1016/S0140-6736(18)32984-2.